The EMBO Journal (2009) 28, 686–696 | © 2009 European Molecular Biology Organization | Some Rights Reserved 0261-4189/09
www.embojournal.org

THE EMBO JOURNAL

EMBO open

Snail1 controls bone mass by regulating *Runx2* and *VDR* expression during osteoblast differentiation

Cristina A de Frutos[1], Romain Dacquin[2,3], Sonia Vega[1,3], Pierre Jurdic[2], Irma Machuca-Gayet[2] and M Angela Nieto[1,*]

[1]Instituto de Neurociencias, CSIC-UMH, San Juan de Alicante, Spain and [2]Institut de Génomique Fonctionnelle de Lyon, Université de Lyon, CNRS, INRA ENS Lyon + IFR 128, Biosciences Lyon-Gerland, Lyon, France

Bone undergoes continuous remodelling throughout adult life, and the equilibrium between bone formation by osteoblasts and bone resorption by osteoclasts defines the final bone mass. Here we show that Snail1 regulates this balance by controlling osteoblast differentiation. Snail1 is necessary for the early steps of osteoblast development, and it must be downregulated for their final differentiation. At the molecular level, Snail1 controls bone mass by repressing the transcription of both the osteoblast differentiation factor *Runx2* and the *vitamin D receptor* (*VDR*) genes in osteoblasts. Sustained activation of Snail1 in transgenic mice provokes deficient osteoblast differentiation, which, together with the loss of vitamin D signalling in the bone, also impairs osteoclastogenesis. Indeed, the mineralisation of the bone matrix is severely affected, leading to hypocalcemia-independent osteomalacia. Our data show that the impact of Snail1 activity on the osteoblast population regulates the course of bone cells differentiation and ensures normal bone remodelling.

The EMBO Journal (2009) **28,** 686–696. doi:10.1038/emboj.2009.23; Published online 5 February 2009
Subject Categories: chromatin & transcription; differentiation & death
Keywords: bone remodelling; osteoblasts; osteoclasts; Runx2; snail; VDR

Introduction

The integrity of the bone depends on the balance between bone resorption by osteoclasts and bone formation by osteoblasts (Karsenty and Wagner, 2002). Indeed, imbalances between these two processes lead to a number of diseases (Rodan and Martin, 2000). Although increased bone mass may be due to osteoclast dysfunction (osteopetrosis) or to high osteoblast activity (osteosclerosis), a reduction in bone mass is usually caused by increased osteoclast number or activity, sometimes accompanied by suppression of osteoblast activity (osteoporosis). Defective mineralisation of the bone matrix associated with defects in the vitamin D signaling leads to osteomalacia. In addition, osteoclast differentiation directly depends on osteoblast activity (Boyle *et al*, 2003), as they secrete osteoclastogenic factors, such as the receptor for activation of nuclear factor kappa B ligand (RANKL), macrophage colony stimulating factor (M-CSF) and osteoprotegerin (OPG) (Lagasse and Weissman, 1997; Lacey *et al*, 1998). Thus, a tight control of osteoblast differentiation is necessary to ensure the appropriate balance between bone formation and bone resorption in the adult.

Runx2 is the main transcriptional regulator of osteoblast differentiation. It is required for both the commitment of mesenchymal cells to the osteoblast lineage and the late stages of osteoblast differentiation and bone mineralisation (Ducy *et al*, 1997; Komori *et al*, 1997; Otto *et al*, 1997; Nakashima and de Crombrugghe, 2003; Xiao *et al*, 2005). Although the mechanisms that control Runx2 activity at the post-translational level are already known (Bialek *et al*, 2004; Jones *et al*, 2006), regulators of its transcription in osteoblasts remain to be identified.

Snail genes are transcriptional repressors best known by their ability to trigger the epithelial to mesenchymal transition (EMT), endowing epithelial cells with motility and invasive properties (Barrallo-Gimeno and Nieto, 2005; Peinado *et al*, 2007). In addition to the regulation of cell movements and adhesion, Snail factors have a broad spectrum of biological functions, including the regulation of cell proliferation and survival (Vega *et al*, 2004). Interestingly, Snail also functions in non-epithelial cells, such as chondrocytes, where it is unable to induce EMT but still controls proliferation. Indeed, its deregulated expression in the developing bone leads to achondroplasia in transgenic mice, the most common form of dwarfism in humans (de Frutos *et al*, 2007). Achondroplasias are associated with activating mutations in FGFR3, which signal in a ligand-independent manner to impair chondrocyte proliferation and differentiation (Ornitz and Marie, 2002). Snail1 is the transcriptional effector of FGFR3 signaling during bone development and disease, and its activity can be inversely correlated with the length of the long bones (de Frutos *et al*, 2007). As in other tissues, Snail1 expression is very tightly regulated in the bone, and thus, we wondered whether its aberrant activation in the adult had any impact on bone homeostasis. Indeed, our data

*Corresponding author. Instituto de Neurociencias, CSIC-UMH, Avda. Ramón y Cajal s/n, San Juan de Alicante 03550, Spain.
Tel.: +34 965 919243; Fax: +34 965 91 95 61;
E-mail: anieto@umh.es
[3]These authors contributed equally to this work

Received: 19 September 2008; accepted: 13 January 2009; published online: 5 February 2009

highlight the fundamental role of Snail1 in controlling bone mass by acting as a repressor of both *Runx2* and *VDR* transcription during osteoblast differentiation.

Results

Sustained Snail1 activation in osteoblasts leads to osteomalacia in transgenic mice

We showed recently that Snail1 activity regulates longitudinal bone growth by controlling chondrocyte proliferation and differentiation (de Frutos *et al*, 2007). However, Snail1 transcripts are also found in the perichondral area (Supplementary Figure 1A), suggesting that it might also be expressed by osteoblasts. Indeed, we have found intense Snail1 expression in osteoblasts from mouse calvaria (Figure 1A). As Snail transcription factors are pleiotropic proteins involved in different cellular processes depending on the cell context (Barrallo-Gimeno and Nieto, 2005), we examined whether Snail1 might also fulfil additional roles in bone formation. To address this issue, we took advantage of our conditional transgenic mouse model in which Snail1 could be activated in the developing bones (Snail1-ER; de Frutos *et al*, 2007; see also Materials and methods and Supplementary Figure 1). To avoid interference with the effects of Snail1 on longitudinal bone growth (de Frutos *et al*, 2007), we have only analysed adult animals here. In this model, constitutively expressed exogenous Snail1 protein only becomes active on nuclear translocation induced by tamoxifen administration. Accordingly, the transgenic Snail1-ER protein was expressed in the osteoblasts of both the trabecular and the cortical bones, and it was efficiently translocated to the nucleus on tamoxifen administration (Supplementary Figure 1B). On Snail1 activation, cartilage-bone staining highlighted deficiencies in the ossification of the long bones in these mice as assessed by Von Kossa staining (Figure 1C and D and Supplementary Figure 2). The images shown in Figure 1C and D are representative of the phenotype observed in around two thirds of the Snail1-ER tamoxifen-treated mice (20 mice analysed per condition in four independent experiments). Cortical thickness was not affected as assessed in Van Gieson stained transverse sections of the tibias (not shown). In the vertebrae, around 15% of the matrix was not calcified (Figure 1B, E and F). The histomorphometric analysis also revealed that when total bone volume was considered as both mineralised bone and osteoid, as established previously (Parfitt *et al*, 1987), the total bone volume

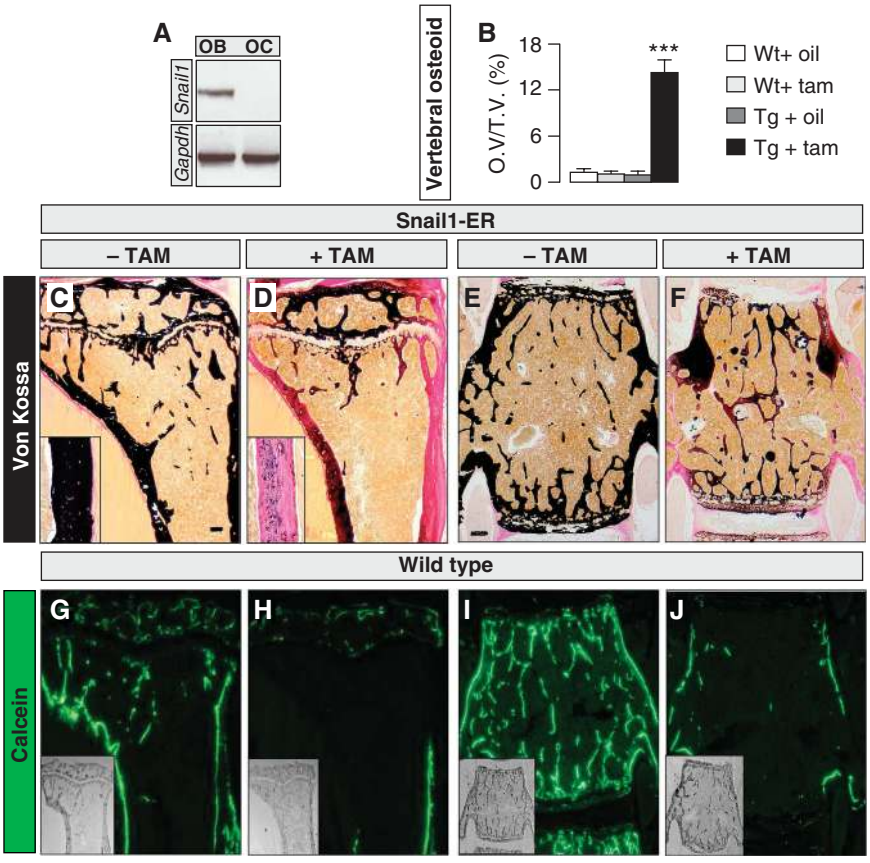

Figure 1 Snail1 activation induces a bone mineralisation defect in adult transgenic mice. (**A**) RT–PCR showing Snail expression in osteoblasts (OB) but not in osteoclasts (OC). (**B**) Percentage of osteoid volume versus total bone volume (OV/TV) determined histomorphometrically in vertebrae ($n=5$). (**C**, **D**) Von Kossa staining of sections of long bones from 16-week-old Snail1-ER transgenic mice shows defective mineralisation as assessed by the deficit in calcium salt deposits (black staining) after 8 weeks of tamoxifen administration. Insets show higher magnification of the cortical bone regions. (**E**, **F**) Von Kossa staining of vertebral sections. Scale bars, 1 mm, ANOVA analysis (***) $P<0.001$. (**G**–**J**) (G, H) Calcein labelling of WT tibiae showing that virtually all trabecular and cortical bone was labelled after 8 days of injections, whereas 2 months after the end of the treatment, labelling was not detectable in the trabeculae and in cortical area located below the growth plate. (I, J) Similar results were obtained in vertebrae in which only scarce calcein labelling was detectable in cortical bone and in the trabecular area 2 months after the end of the treatment.

did not significantly change (Supplementary Figure 3). Similarly, the trabeculae were similar in number and thickness (Supplementary Figure 3). The deficient mineralisation was more severe in the tibia than in the vertebrae and indeed, in around 20% of the treated animals the majority of the cortex and some trabeculae were composed of only osteoid tissue 2 months after Snail1 activation commenced. As the mice had well mineralised bones before tamoxifen administration, it appears that bone remodelling is very rapid. To confirm this, we analysed the rate of remodelling in wild-type mice by injecting calcein for 8 consecutive days into wild-type mice, and assessing the labelling that remained at different time points. This labelling had decreased 1 month after the injection (not shown), and it was greatly diminished after 2 months, particularly in the tibia and the vertebrae (Figure 1G–J). Hence, the strong phenotype that we observed in our transgenic mice was compatible with Snail1 inducing a defect in bone formation, and on the other hand, it is very reminiscent of osteomalacia or defective bone mineralisation (Karsenty and Wagner, 2002).

Snail1 represses VDR transcription in osteoblasts and impairs osteoclastogenesis

Osteomalacia has been associated with a deficit in vitamin D or its signalling through the VDR receptor (Li *et al*, 1997; Yoshizawa *et al*, 1997). However, the primary role of vitamin D signalling in bone mineralisation is to stimulate intestinal absorption of calcium. Indeed, dietary restoration of mineral ion homeostasis prevents osteomalacia in VDR mutant mice (Li *et al*, 1998; Amling *et al*, 1999). As Snail1 directly represses the transcription of the *Vdr* gene in human colon cancer cells (Palmer *et al*, 2004; Pena *et al*, 2005), the osteomalacia phenotype of Snail1-ER mice could be due to a deficient VDR expression in the intestine and low calcium absorption. However, as the Snail1-ER transgenic protein was not expressed in the intestine, this does not appear to be the case (Supplementary Figure 4A–E). Consequently, VDR protein expression and distribution as well as the morphology of the intestine were unaffected by tamoxifen administration (Supplementary Figure 4F–M). Consistent with this finding, calcium and phosphate serum levels were normal in the Snail1-ER tamoxifen-treated mice (Figure 2A and B). Moreover, serum levels of creatinine and urea (not shown) were also unaffected, indicating that tamoxifen administration to Snail1-ER mice did not affect the kidneys, as might be expected from the very low levels of transgenic protein in the kidney (not shown). Although the serum levels of alkaline phosphatase were elevated in the tamoxifen-treated mice (Figure 2C), this increase was very modest compared with that observed in VDR mutants (Yoshizawa *et al*, 1997; Panda *et al*, 2004). Interestingly, we also found normal serum levels of the vitamin D_3 precursor $25(OH)D_3$ (Figure 2D) and normal expression levels of its hydroxylase Cyp27b1 in both kidney and bone (Figure 2E and F).

Although an ion-rich diet can rescue osteomalacia in *VDR* mutant mice, the number of osteoclasts remains low because VDR signalling is also required in osteoblasts for osteoclast differentiation (Panda *et al*, 2004). As such, VDR is also expressed in osteoblasts, where it directly activates the promoter of the osteoclast differentiation factor RANKL and downregulates the expression of OPG, a decoy RANKL receptor that inhibits osteoclastogenesis (Simonet *et al*, 1997;

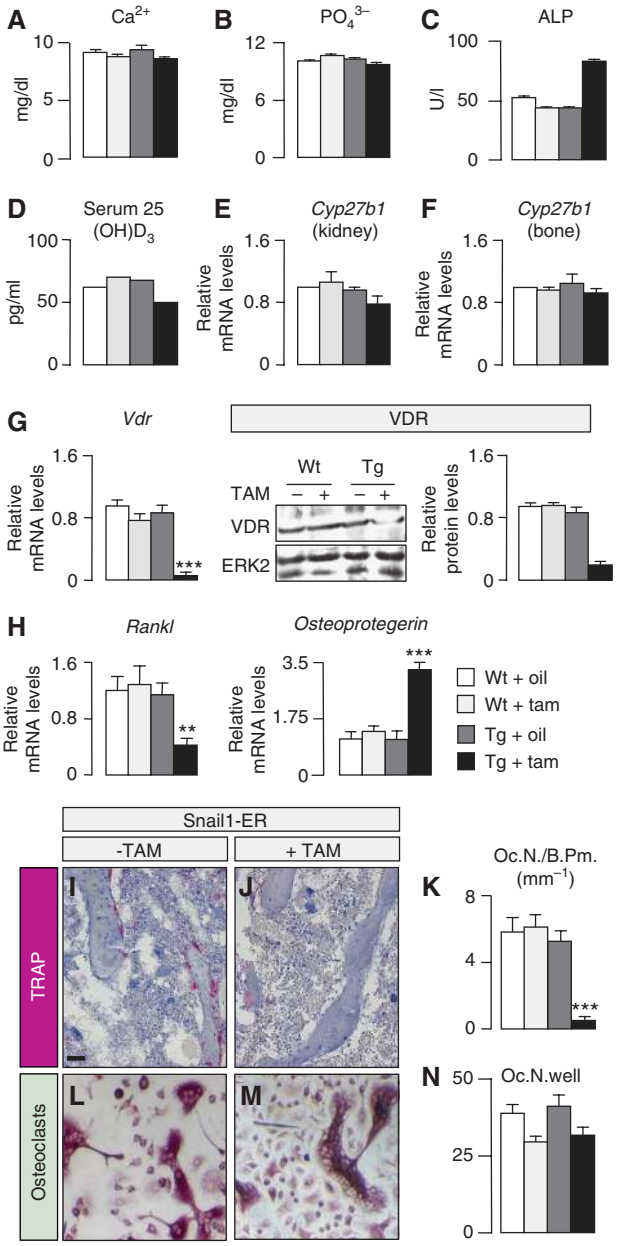

Figure 2 Aberrant Snail1 activation impairs osteoclastogenesis. Calcium (**A**), phosphate (**B**), alkaline phosphatase (ALP, **C**) and $25(OH)D_3$ (**D**) concentrations in serum samples from 16-week-old mice after 8 weeks of corn oil or tamoxifen administration. The results are expressed as the means ± s.d. from five samples. (**E**, **F**) The $25(OH)D_3$ hydroxylase Cyp271b is unaltered in both the kidney and the bone of Snail1-ER transgenic mice regardless of whether tamoxifen is administered. (**G**) Snail1 activation inhibits vitamin D receptor mRNA expression and protein accumulation. (**H**) Snail1 activation is also accompanied by a decrease in the expression of the *Rankl* osteoclastogenic factor and an increase in that of the osteoclastogenesis inhibitor *Osteoprotegerin*. The results are expressed as the mean ± s.d. from three independent experiments carried out on limbs obtained from 16-week-old Snail1-ER mice after 8 weeks of treatment with tamoxifen. (**I**, **J**) Osteoclasts are revealed by tartrate-resistant acid phosphatase (TRAP) staining. Sections are counterstained with alcian blue. (**K**) Quantification of the osteoclast population by histomorphometric analysis of bones from 16-week-old wild-type and Snail1-ER mice ($n = 10$). (**L**–**N**) Osteoclast differentiation in culture is not affected by Snail1 activation. Oc.N., osteoclast number; B.Pm., bone perimeter. Scale bar, 100 μm. ANOVA analysis, $^{**}P < 0.01$ and $^{***}P < 0.001$.

Kitazawa *et al*, 2003; Kondo *et al*, 2004). We examined whether Snail1 could repress *Vdr* transcription in the bone as it does in colon cancer cells, and we found that Snail1 activation on tamoxifen administration did indeed repress of both *Vdr* transcription and protein accumulation (Figure 2G). This inhibition of *Vdr* expression impairs the activation of *Rankl* expression and increases *Osteoprotegerin* levels (Figure 2H), which could explain the reduction observed in the osteoclast population (Figure 2I–K). We also examined the chondrocytes, as the deletion of VDR in these cells also provokes a reduction in osteoclastogenesis due to decreased RANKL expression (Masuyama *et al*, 2006). Tamoxifen did not affect *Rankl* expression (not shown) in chondrocytes differentiated from dissociated 14.5 dpc hindlimb cells obtained from transgenic embryos as described previously (de Frutos *et al*, 2007). Finally, although endogenous *Snail1* is not expressed in the osteoclast population (Figure 1A), we examined whether the transgenic protein might be expressed in these cells, possibly contributing to the impaired osteoclast differentiation observed in the Snail1-ER mice treated with tamoxifen. Transgenic osteoclasts do not express Snail1-ER (not shown) and their differentiation in cultures was similar in wild-type and transgenic animals, although tamoxifen seemed to slightly decrease the efficiency of the process in both cases (Figure 2L–N). Together, these data indicate that on the one hand, the impaired osteoclastogenesis was due to the defects in VDR signalling in osteoblasts that diminished the availability of RANKL, and on the other hand, that there is no cell-autonomous defect in the osteoclast population or defects in VDR signalling in chondrocytes. Thus, with respect to VDR signalling, the Snail1-ER mice represent an osteoblast-specific model for VDR deficiency.

Transient Snail1 expression is required for osteoblast differentiation

Although bone-specific repression of *VDR* transcription by Snail1 can explain the defects in osteoclastogenesis in the transgenic mice, it cannot account for the defective mineralisation given that ion homeostasis is maintained. Thus, we decided to assess the rate of bone formation by examining calcein incorporation after its injection *in vivo*. The strong impairment in calcein apposition observed was compatible with the defective mineralisation observed in these bones (Figure 3A and B), and suggesting that the osteoblasts failed to fully differentiate. Indeed, the bones from Snail1-ER tamoxifen-treated mice expressed higher levels of *Collagen I* transcripts and lower levels of *Osteocalcin* expression in Snail1-ER bones (Figure 3C and E), markers of early and late osteoblast differentiation, respectively (Nakashima and de Crombrugghe, 2003), while the number of osteoblasts remained similar (Figure 3F and G).

To examine the role of Snail1 in osteoblast differentiation, we developed an *in vitro* system from embryonic bones in which the stages of proliferation, differentiation and mineralisation could be followed. This culture system accurately reproduced the differentiation pattern described previously (Maes *et al*, 2007), in terms of osteoblasts differentiated from wild-type embryos or from transgenic Snail1-ER embryos in the absence of tamoxifen (Figure 4A–C). We found that *Snail1* was transiently expressed in a profile that closely resembled that of *Collagen I*, probably reflecting the indirect induction of *Collagen I* expression by Snail1 as occurs in

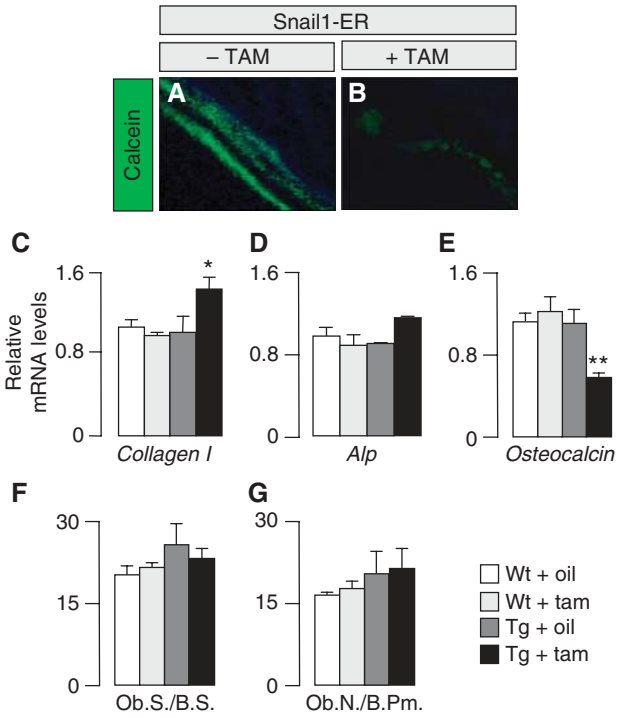

Figure 3 Aberrant Snail1 activation impairs calcein apposition. (**A**, **B**) Mineral apposition was visualised after calcein injection ($n=5$ per group). (**C**–**E**) Snail1 activation increases the transcription of the early differentiation osteoblast markers *Type I Collagen* and *alkaline phosphatase* (*Alp*; only a slight increase) and decreases that of the differentiated population marker *Osteocalcin*. Real-time PCR was carried out on limbs obtained from 16-week-old Snail1-ER mice after 8 weeks of treatment with tamoxifen. The results are expressed as mean ± s.d. from three independent experiments. (**F**, **G**) The number of osteoblasts per bone perimeter is unaltered on Snail1 activation. Histomorphometric analysis of bones from 16-week-old wild-type and Snail1-ER mice ($n=10$). Ob.S., osteoblast surface; Ob.N., osteoblast number; B.S., bone surface; B.Pm., bone perimeter. ANOVA analysis, $^{*}P<0.1$ and $^{**}P<0.01$.

kidney epithelial cells (Boutet *et al*, 2006). The expression of phospho-histone 3, p21 or p27 was not altered when cells from transgenic embryonic bones differentiated to osteoblasts in the presence of tamoxifen, indicating that unlike in chondrocytes (de Frutos *et al*, 2007), Snail1 does not affect osteoblast proliferation (Supplementary Figure 5).

Transgenic Snail1 activation by nuclear translocation on tamoxifen administration (Figure 4D) was correlated with cell commitment to the osteoblast lineage. Mesenchymal cells were converted into immature osteoblasts as they expressed *Osteopontin* and upregulated *Collagen I* expression (Komori, 2008). However, sustained Snail1 activation prevented them from continuing their differentiation (Figure 4E). Significantly, the normal maturation process was recovered on Snail1 inactivation due to its cytoplasmic relocalisation after tamoxifen removal. *Collagen I* and *Osteopontin* expression were downregulated, and the transcription of the *Bone Sialoprotein*, *Osteocalcin*, *Dentin matrix protein 1* (*Dmp1*) and the transmembrane endopeptidase *Phex* began to increase (Figure 4F and G; see also Supplementary Figure 6). The expression of *ATF4*, an osteoblast marker not regulated at the transcriptional level, was unaltered regardless of the state of Snail1 activity (Supplementary Figure 6). In summary, our data indicate that although Snail1 downregulation was

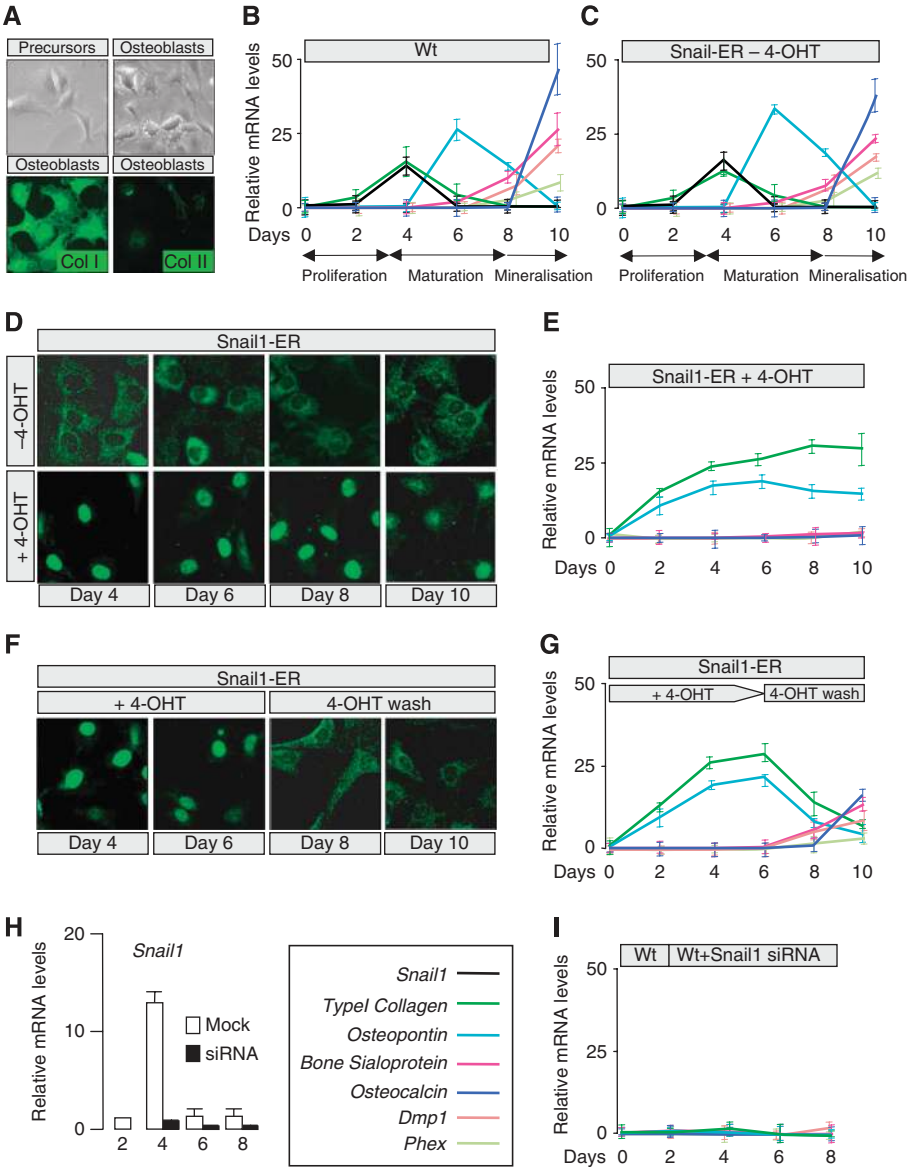

Figure 4 Snail1 is necessary for the early steps of osteoblast differentiation, and its downregulation is required for terminal differentiation. (**A**) Primary cultures of wild-type mesenchymal limb cells differentiate into osteoblasts, as confirmed by the expression of the *Type I Collagen* osteoblast marker and the absence of the *Type II Collagen* chondrocyte marker. (**B**, **C**) Relative mRNA expression of *Snail1* and the *Type I Collagen*, *Osteopontin*, *Bone Sialoprotein*, *Osteocalcin*, *Dentin matrix protein 1* (*Dmp1*) and the transmembrane endopeptidase *Phex* during osteoblast differentiation in culture of wild-type and Snail1-ER transgenic mesenchymal cells, respectively. (**D**, **E**) Snail1 activation prevents osteoblast differentiation in culture. Note the nuclear translocation and ensuing Snail1 activation on tamoxifen administration. (**F**, **G**) Osteoblast differentiation occurs *in vitro* in cultures in which tamoxifen was washed out after 6 days of administration, showing the reversibility of the treatment. Note that Snail1 nuclear translocation is only observed in the presence of 4-OH-Tamoxifen. (**H**) Snail1 siRNA transfection almost completely blocks *Snail1* expression as assessed by real-time RT–PCR. (**I**) Snail1 silencing prevents osteoblast differentiation, as assessed by the absence of early differentiation markers. *Snail1* (black), *Type I Collagen* (green), *Osteopontin* (sky blue), *Bone Sialoprotein* (fuchsia), *Osteocalcin* (navy blue), *Dmp1* (light brown) and *Phex* (light green).

necessary for osteoblast differentiation, it might be required for the initial steps in the differentiation process. To assess whether this was indeed the case, Snail1 siRNA was transfected into wild-type primary cultures derived from 14.5 dpc embryonic hindlimbs at the time of endogenous Snail1 induction. Snail1 was almost totally silenced (Figure 4H) and differentiation was completely abolished (Figure 4I). Thus, Snail1 is necessary at early stages of osteoblast differentiation and must be downregulated for differentiation and mineralisation to proceed. Given the role of Snail1 in osteoblast differentiation, it is likely that it also contributes to intramembranous ossification.

Snail1 directly controls Vdr and Runx2 transcription during osteoblast differentiation

Having determined that Snail1 regulates osteoblast differentiation in culture, and given that it is a transcription factor, we set out to define its targets. Having shown that VDR expression was inhibited in bones when Snail1 was activated, we analysed *Vdr* expression in our osteoblast differentiation

system. As expected, *Vdr* expression inversely correlated with that of *Snail1* (Figure 5A) and, furthermore, its transcription remained repressed in the presence of activated Snail1 (Figure 5B). As Snail1 directly inhibits *Vdr* transcription in colon cancer cells as assessed in promoter activity assays (Palmer *et al*, 2004), we examined whether it could also bind to its promoter in osteoblasts. Three consensus E-boxes for Snail binding exist in a 0.5-kb fragment upstream of the *Vdr* coding region (Cano *et al*, 2000; Figure 5C). Chromatin immunoprecipitation (ChIp) analyses of osteoblasts from Snail1-ER transgenic mice confirmed that Snail1-ER can bind to boxes II and III and as expected, only in the presence of tamoxifen (Figure 5C). In these ChIp experiments, the ER-antibody was used to detect only the exogenous Snail1-ER fusion protein and not the endogenous Snail1 that would bind to the promoter in the presence or absence of tamoxifen administration. These data confirm that Snail1 also binds directly to the *Vdr* promoter in osteoblasts.

Besides *VDR*, *Runx2* was a clear candidate target to examine, as it is considered the main regulator of osteoblast differentiation, and it is first required for the commitment of mesenchymal cells to the osteogenic and osteoblast lineage (Ducy *et al*, 1997; Komori *et al*, 1997; Otto *et al*, 1997; Nakashima and de Crombrugghe, 2003). Later on, Runx2 is also required for the conversion of these cells to mature osteocytes and for the expression of mineralisation proteins (e.g., osteocalcin; Xiao *et al*, 2005). We analysed *Runx2* expression in our osteoblast differentiation system and as for *Vdr*, *Runx2* transcription was inversely correlated with that of *Snail1* (Figure 5D). This relationship suggested that Snail1 might repress *Runx2*, compatible with the repression of *Runx2* observed in transgenic osteoblasts cultured in the presence of tamoxifen (Figure 5E). Furthermore, Snail1 transfection in differentiating osteoblasts induced sustained repression of *Runx2* transcription (Figure 5F), although *Runx2* was expressed strongly after transfection of a Snail1 siRNA (Figure 5F). These data indicate that Snail1 may act as a *Runx2* repressor, and this led us to assess whether Snail1 could directly repress *Runx2* promoter activity.

Nine consensus E-boxes for Snail binding exist in an 8-kb fragment upstream of the *Runx2* coding region (Figure 6A). However, only the two most proximal boxes were conserved between human and mouse. Using a reporter construct that included these two boxes, we found that Snail1 decreased the activity of the *Runx2* promoter in osteoblasts (Figure 6A; construct 1). Although deletion or mutations of the distal E-box of this pair (constructs 2 and 5) did not affect repressor activity, deletion or mutations in the most proximal box significantly relieved the repression of the *Runx2* promoter (Figure 6A; constructs 3 and 4). Moreover, simultaneous mutations in the two boxes completely abrogated inhibition. The sequences deleted in construct number 3 (Figure 6A) are likely to contain binding sites for Runx2 activators, as its activity in the absence of Snail1 is much lower than that of the control fragment (construct 1). Together, these data indicate that the binding of Snail1 to the most proximal box is sufficient to inhibit *Runx2* promoter activity and that the second box cooperates in this repression.

A similar ChIp analysis of osteoblasts from Snail1-ER transgenic mice confirmed that like the *Vdr* promoter, Snail1-ER can also only bind to these two conserved boxes in the *Runx2* promoter in the presence of tamoxifen (Figure 6B). Interestingly, Snail1 is unable to bind to four additional consensus boxes or to the three perfect-match E-boxes contained in 3 kb or between 7 and 8 Kb fragments upstream of the *Runx2* coding region, respectively (Figure 6B and Supplementary Figure 7).

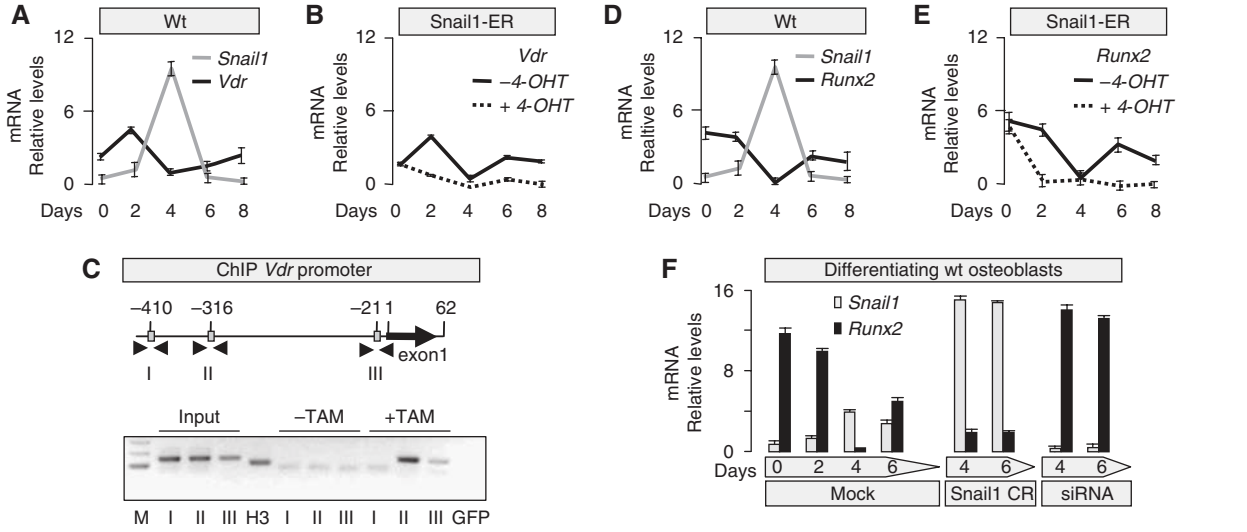

Figure 5 Snail1 directly regulates *Vdr* and *Runx2* expression during osteoblast differentiation in culture (**A**) The levels of *Snail1* and *Vdr* expression are inversely correlated during osteoblast differentiation. (**B**) Sustained activation of Snail1 after 4-OHT administration maintains low *Vdr* expression. (**C**) Chromatin immunoprecipitation (ChIP) assays carried out on osteoblasts differentiated from Snail1-ER transgenic mice confirm that Snail1 only binds to boxes II and III in the *Vdr* promoter on tamoxifen administration. M, fragment length markers; input material was tested for each primer set (boxes I, II and III); H3, positive control of the immunoprecipitate, the sample was immunoprecipitated with anti-H3 antibody and amplified with *Gapdh* primers; GFP, negative control of the immunoprecipitate, the sample was immunoprecipitated with anti-GFP antibody and amplified with *Gapdh* primers. (**D**, **E**) The levels of *Snail1* and *Runx2* expression are also inversely correlated during osteoblast differentiation, and similarly, sustained Snail1 activation maintains *Runx2* expression inhibited. (**F**) When osteoblast primary cultures were transfected with a plasmid containing the coding region of Snail1 (Snail1 CR), *Runx2* expression was very weak, whereas transfection with a Snail1 siRNA led to stable and strong *Runx2* expression.

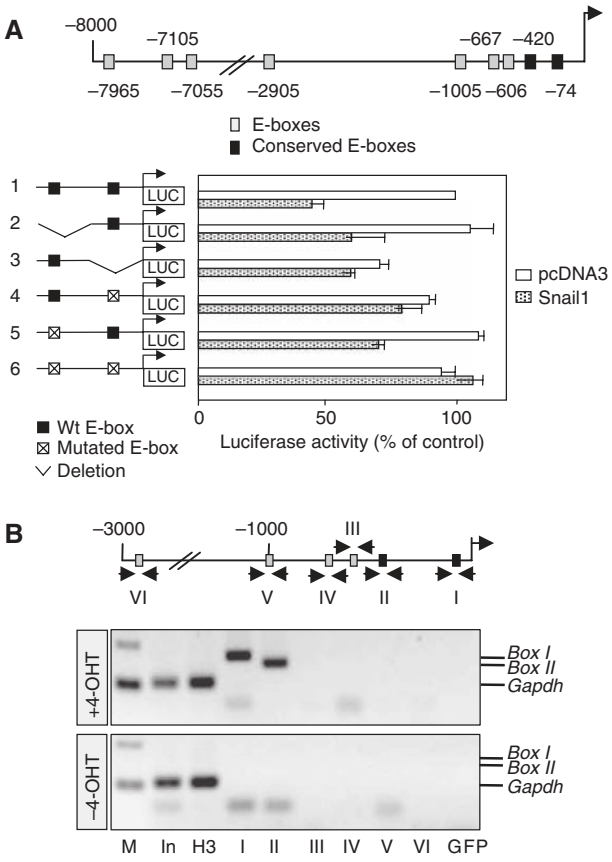

Figure 6 Snail1 is a direct repressor of *Runx2* transcription. (**A**) Diagram of the 8-kb region upstream of the translational initiation site in the mouse *Runx2* gene showing the putative sites for Snail1 binding (E-boxes). Two of these boxes are conserved in the human (black squares). Luciferase reporter constructs carrying the wild-type *Runx2* promoter or deletions/mutations in the two conserved E-boxes were assayed in osteoblasts together with either the mouse Snail1 expression vector or an empty vector as a control (pcDNA3). Luciferase activity was measured 24 h after transfection, and the activity was expressed relative to that of the wild-type construct. The results are expressed as the mean values ± s.e. of duplicates from four independent experiments. Snail1 repressed the activity of the wild-type *Runx2* promoter, but it did not affect the promoter constructs in which the most proximal conserved E-box was deleted or mutated. (**B**) Chromatin immunoprecipitation (ChIP) assays carried out in osteoblasts differentiated from Snail1-ER transgenic mice confirm that Snail1 only binds to these two conserved proximal E-boxes and only on tamoxifen administration. M, fragment length markers; In (the input material), immunoprecipitation positive control H3 (sample immunoprecipitated with anti-H3 antibody) and immunoprecipitation negative control GFP (sample immunoprecipitated with anti-GFP antibody) were tested with GAPDH primers. The input material was also tested for each primer set corresponding to the fragments containing all the putative binding sites (see Supplementary Figure 7).

Although our culture system reproduced the described pattern of osteoblast differentiation, we decided to analyse whether Snail1 also behaved as a Runx2 repressor *in vivo*. We first examined the endogenous pattern of *Snail1* expression in the perichondral area of mouse embryos throughout fetal development. We found that *Snail1* expression was very dynamic, and that it followed a similar profile to that found in our cultures, with a peak of high expression at 16.5 dpc (Figure 7C). Interestingly, *Snail1* expression was inversely correlated with that of *Runx2* both in the perichondral area and in the trabecular bone (Figure 7A–J). These data are compatible with the repression of *Runx2* by Snail1. As such, we also found that *Runx2* is repressed in Snail1-ER transgenic bones on Snail1 activation *in vivo* (Figure 7K–N). In addition, the direct downstream target of Runx2, *Osterix* (Nakashima *et al*, 2002; Nishio *et al*, 2006), was also inhibited on Snail1 activation in these bones (not shown). These data validate the specificity of the transfection and ChIp assays and confirm that Snail1 directly binds to the *Runx2* promoter and represses its transcription during osteoblast differentiation.

Discussion

We have shown that Snail1 directly represses both *VDR* and *Runx2* transcription during osteoblast differentiation. The transitory expression of Snail1 in osteoblasts can control the course of differentiation by facilitating an early and a late phase of Runx2 activity. Sustained activation of Snail1 in mice stabilises the normally transient repression of transcriptional cascades downstream of *Runx2* and *Vdr* in osteoblasts, inducing defective mineralisation and impairing osteoclastogenesis, respectively. When coupled with the Snail1-mediated induction of *Collagen I*, these alterations generate uncalcified matrix or osteoid and thus, osteomalacia independent of hypocalcemia and hypophosphatemia.

Despite the *in vivo* data obtained in this study come from a transgenic mouse model overexpressing Snail1, we believe that it significantly helps understand the mechanisms that control bone formation and resorption. It reveals an unexpected and important role of Snail1 in osteoblast differentiation in culture, which is compatible with the data obtained in transgenic mice (Figure 8). Although our model is not osteoblast specific, we have ruled out the cell-autonomous contribution of chondrocytes or osteoclasts in these processes in our mice. On the one hand, Snail1-ER protein is not expressed in osteoclasts, and on the other hand, we have not seen any defect in chondrocytes that could explain the observed phenotype. We show that Snail1 controls *Vdr* expression in osteoblasts. It is known that impaired *Vdr* signalling in the intestine leads to osteomalacia due to defective calcium absorption in the intestine. However, Snail1 cannot be associated with VDR signalling or calcium uptake in the intestine in healthy conditions, as Snail1 is not endogenously expressed in normal intestinal tissue. Similarly, this transgenic line of Snail1-ER mice does not express Snail1 in the intestine either and maintained normal VDR expression and serum ion levels. Thus, with respect to VDR signalling, Snail1-ER mice provide an osteoblast-specific defective model, where Snail1-mediated repression of *Vdr* transcription in osteoblasts leads to defects in osteoclastogenesis due to the consequent deregulation of *Rankl* and *Osteoprotegerin*. Interestingly, Snail1 is aberrantly activated in colon cancer cells, where it represses *Vdr* expression (Palmer *et al*, 2004), as it normally occurs in osteoblasts (this work). Perhaps the benefits of a higher calcium intake associated with a reduced risk of colon cancer detection (Wu *et al*, 2002) can be related to a compensation of deficient calcium uptake in patients with impaired VDR signalling after aberrant activation of Snail1 as part of the transformation process.

Importantly, our studies also help to clarify the temporal regulation of *Runx2* transcription during normal bone development and homeostasis. Undifferentiated mesenchymal

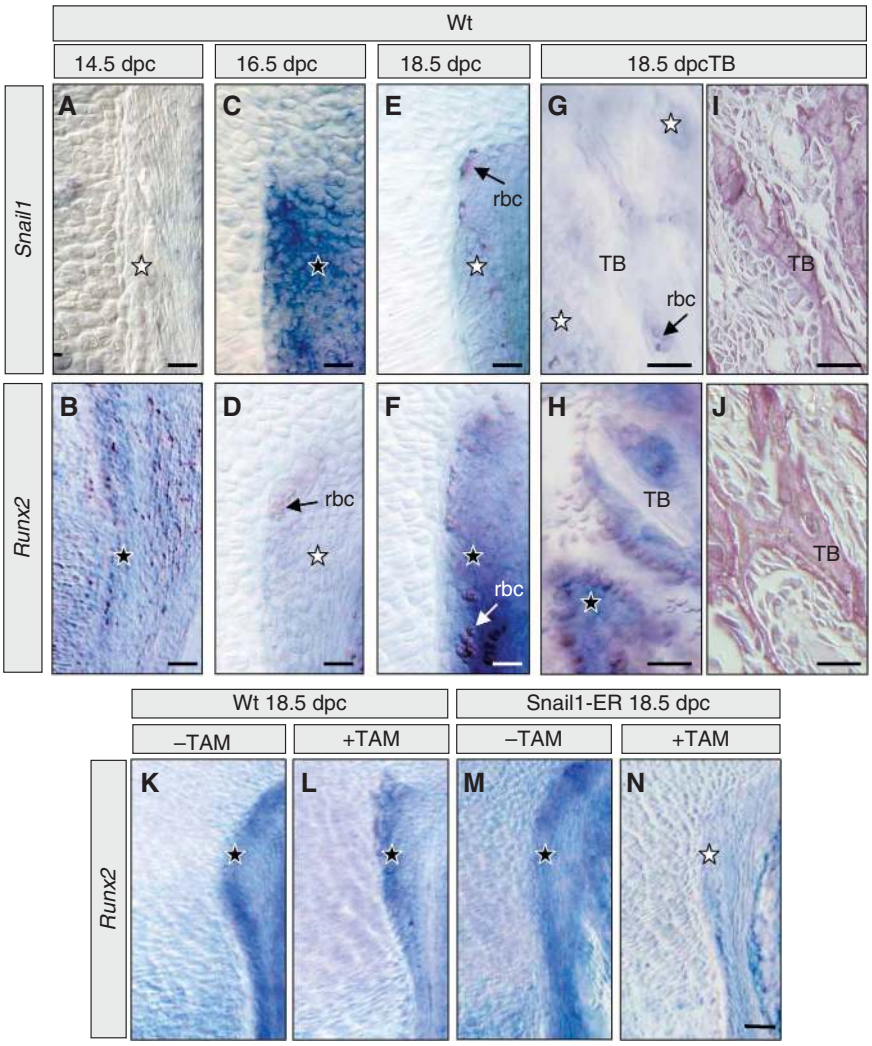

Figure 7 Snail1 activation represses *Runx2* expression *in vivo*. (**A–J**) *Snail1* and *Runx2* show excluding expression patterns during osteoblast differentiation *in vivo* in wild-type mice. (A, B) At 14.5 dpc, only *Runx2* is expressed in the perichondrium and in the periosteum (not shown). (C, D) *Snail1* is expressed in the perichondrium at 16.5 dpc while *Runx2* transcripts are absent. (E, F) At 18.5 dpc, *Snail1* expression has decreased in the perichondrium, whereas that of *Runx2* has significantly increased. (G, J) At the same stage, *Runx2* is expressed in the osteoblasts surrounding the trabecular bone (TB) in the absence of *Snail1* transcripts. (**K–N**) Snail1 activation by tamoxifen administration inhibits *Runx2* expression in the perichondrium of Snail1-ER transgenic mice. Black and white stars indicate high and low expression levels, respectively. Arrows point to unspecific signal observed in red blood cells (rbc). Black stars indicate endogenous *Runx2* expression, and white star indicate repression of endogenous *Runx2* expression by Snail1 activation.

cells have low levels of *Snail1*, allowing the expression of *Runx2* transcripts. However, Runx2 activity is low at these early stages due to its interaction with Twist proteins, which prevent the Runx2 protein from binding to its target promoters (Bialek *et al*, 2004). When Twist is downregulated, Runx2 becomes functional and by blocking adipocyte and chondrocyte differentiation, it activates osteoblast formation. It is known that Runx2 must be later suppressed for immature osteoblasts to continue differentiating (Komori, 2008), and later on, it needs to be re-expressed as it is essential for terminal differentiation into osteocytes and complete mineralisation (Stein *et al*, 2004; Xiao *et al*, 2005). Our data showing the transient nature of Snail1 expression during osteoblast differentiation and its ability to act as a direct transcriptional repressor of *Runx2*, provide an explanation for this complex dynamics of Runx2 expression throughout the differentiation process. As such, at the time when Runx2 has specified the osteoblast phenotype, Snail1 is activated and transiently represses *Runx2* so that differentiation to the immature osteoblast can proceed. In addition to inhibiting *Runx2* expression, Snail1 actively favours the formation of immature osteoblasts, as it is necessary for *Collagen I* and *Osteopontin* expression (Figure 4H) and represses the expression of the mineralisation genes *Phex* and *Dmp1*. Subsequent Snail1 downregulation releases *Runx2* transcriptional repression and allows mineralisation to proceed, as this second wave of *Runx2* expression is necessary to activate *Bone Sialoprotein* and *Osteocalcin* (Stein *et al*, 2004). On mineralisation, the levels of Runx2 protein are controlled by Schnurri-3, which promotes its degradation in the proteasome (Jones *et al*, 2006).

In conclusion, we have revealed Snail1 to be the first transcriptional repressor of *Runx2*, which together with the post-translational regulation co-ordinated by Twist and

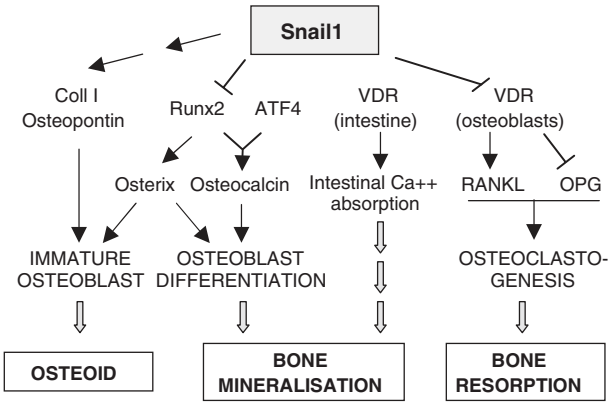

Figure 8 Diagram showing the central position of Snail1 in the bone remodelling pathways. In wild-type mice, Snail1 is necessary for the first steps of osteoblast differentiation in a dual manner. It activates the expression of the early differentiation markers Collagen I and Osteopontin while it inhibits *Runx2* expression, necessary for differentiation to proceed. The transient nature of Snail1 expression allows a second wave of *Runx2* transcription needed for bone mineralisation. On the other hand, Snail also directly represses *Vdr* transcription in osteoblasts providing another link between osteoblastogenesis and osteoclastogenesis. Consequently, sustained Snail1 activation in adult Snail1-ER mice supports the formation of the osteoid but inhibits osteoblast and osteoclast terminal differentiation, leading to a defective mineral deposition.

Schnurri-3 (Bialek *et al*, 2004; Jones *et al*, 2006), controls the complex dynamics of Runx2 protein activity during osteoblast differentiation. Snail1 also favours the synthesis of unmineralised matrix by indirectly activating *Collagen I* expression and it controls osteoclastogenesis by directly repressing *Vdr* transcription. Thus, Snail1 lies upstream of three fundamental pathways in bone remodelling and the control of adult bone mass (Figure 8). Our data indicate that aberrant expression of Snail1 would lead to osteomalacia even under normal ion homeostasis conditions as it occurs in the presence of vitamin D and a wild-type *Vdr* gene. In addition, this study provides further insight into the complex regulation of bone formation and resorption.

Materials and methods

Mice

The Snail-ER^{T2} construct (de Frutos *et al*, 2007) was microinjected into fertilised C57 × CBA hybrid eggs to generate transgenic mice according to Hogan *et al* (1994). A line was selected that expressed significant levels of the transgenic protein in the adult bone, immunohistochemically detecting the transgenic protein with a human estrogen-receptor antibody (Santa Cruz). All mice were killed by cervical dislocation.

Induction with tamoxifen or 4-OH-Tamoxifen

Tamoxifen (Sigma) was dissolved in corn oil at a concentration of 30 mg/ml. Corn oil, alone or containing tamoxifen, was injected intraperitoneally every 2 days. Tamoxifen was injected at a concentration of 200 μg or 75 μg/g of body weight to 8-week-old animals for 8 weeks or to pregnant females at 12.5 and 14.5 dpc, respectively. A 1-mM stock solution of 4-OH-Tamoxifen (Sigma) was prepared in ethanol and further diluted to the appropriate concentrations before its use in cultures.

Embryo dissection and in situ hybridisation

Embryos were dissected at 12.5–18.5 dpc and fixed overnight in 4% paraformaldehyde. Hindlimbs were decalcified in 22.5% formic acid and 10% sodium citrate at 4°C for 24 h and subsequently, they were gelatin-embedded before obtaining 30–50 μm vibratome sections. *In situ* hybridisation was performed as previously described in Cano *et al* (2000), and the plasmids used to obtain digoxigenin riboprobes corresponded to the following cDNA sequences: *Snail1* (1–1600 bp) and *Runx2* (484–650 bp).

Skeleton staining

The hindlimbs were dissected and the skin was removed. The limbs were fixed in 10% formalin, and the cartilage was stained with Alcian Blue. After washing, the limbs were trypsinised and stained with Alizarin Red S (for calcium salts), cleared by KOH treatment and stored in glycerol.

Histology and histomorphometric analyses

Non-decalcified bones were embedded in methylmethacrylate according to standard protocols (Parfitt *et al*, 1987) before processing them for Von Kossa, tartrate resistant acid phosphatase (TRAP) staining or histological analysis. Mice were injected with 100 μl of a calcein solution (5 mg/ml), both 6 and 2 days before they were killed, and they were then processed for plastic embedding as described above. In the bone-remodelling assay, injections were given on 8 consecutive days, and mice were killed 1 week (to confirm labelling efficiency), 1 or 2 months after the last injection. Measurements were performed with the Osteo Measure Analysis System (Osteometrics) using a 3CCD color video DXC-390 camera (Sony) coupled to a microscope (DMLB; Leica). Statistical differences between groups were assessed by the *t*-test.

Immunohistochemistry

Histological sections were prepared from hindlimbs fixed in 10% formalin that were decalcified with 22.5% formic acid in 10% sodium citrate at room temperature for 16 h, and embedded in gelatin. Gelatin sections (100 μm) were stained using an anti-hER antibody (Santa Cruz) diluted 1:200, and they were developed with the ABC reagent (Pierce) according to the manufacturer's instructions. Other histological sections were prepared from tissues fixed in 10% formalin and embedded in paraffin. Paraffin sections (5 μm) were stained with haematoxylin and eosin or subjected to immunohistochemistry with antibodies against either the anti-human estrogen receptor (α-hER, 1:200; Santa Cruz) or anti-VDR (α-VDR, 1:200; Chemicon) antibodies. The appropriate Alexa 488 secondary antibodies were used diluted 1:5000 in 1% BSA in PBS.

Calvaria primary cultures

Osteoblasts were isolated from enzymatically dissociated calvaria from 3-day-old mice, and they were plated in differentiation medium: α-MEM (Invitrogen) containing 10% heat-inactivated serum (Sigma–Aldrich), 50 μg/ml ascorbic acid and 10 mM sodium β-glycerophosphate. After 24 h, the cells were harvested with 0.01% trypsin in PBS, and they were then plated in 35 mm culture dishes at 2×10^4 cells/dish and grown for 22 days in the differentiation medium. Total cellular mRNA was extracted from primary osteoblasts with RNA-Now (Eurobio, Les Ulis, France).

Primary osteoclast cultures

Osteoclast cell cultures were established with spleen cells from 6- to 8-week-old OF1 male mice or Snail1-ER mice, whereby 2500 or 4000 cells/mm^2 were seeded and cultured for 8 days. Bone marrow mononuclear cells from 8-week-old WT or Snail1-ER mice were plated on 96-wells plate at the density ranging from 10^4 cells to 5×10^4 per well, and the following day (D1) treated with 200 nM tamoxifen (Sigma) or vehicle for 6 days. All cultures were carried out in the presence of α-MEM (Invitrogen) containing 10% (v/v) foetal calf serum (FCS, Biowest, Nuaille, France), M-CSF (20 ng/ml) and RANKL (50 ng/ml) from R&D system. Osteoclast differentiation was evaluated by TRAP staining using the leukocyte acid phosphatase kit from Sigma.

Primary osteoblast cultures

Hindlimbs from 14.5 dpc transgenic or wild-type mouse embryos were dissected in medium (α-MEM, 1% BSA, 0.1% L-Glutamine, 0.1% penicillin/streptomycin) and left overnight at 37°C and 5% CO_2. The following day, the bones were trypsinised for 10–15 min at 37°C and digested for 2 h in 3 mg/ml Collagenase P in DMEM with 10% FCS at 37°C. The reaction was inactivated by adding primary culture media (50% F-12, 50% DMEM, 10% FCS, 0.1%

L-Glutamine, 0.1% penicillin/streptomycin), and the cells were plated at a density of 1.5×10^6 cells/P100 in primary culture media (Woods and Beier, 2006). After 5 days in culture, the cells were seeded at a density of 1×10^5 per well and differentiated to osteoblasts in differentiation media (50% F-12, 50% DMEM, 0.1% L-Glutamine, 0.1% penicillin/streptomycin, 10 mM β-glycerophosphate, 100 nM dexamethasone, 0.2 mM ascorbic acid (Reyes *et al*, 2001) in the presence or absence of 200 nM 4-OH-Tamoxifen, and the medium was changed every 2 days. Cells were transfected after 2 days in differentiation medium using Lipofectamine (Invitrogen) with Snail1 siRNA or the random negative control, and/or an expression plasmid containing the Snail1-coding region (CR), RNA was isolated every 2 days using the SIGMA Genelute Mammalian Total RNA Kit according to the manufacturer's instructions. The siRNA duplex oligonucleotide used was described previously (de Frutos *et al*, 2007). Immunofluorescence was carried out using antibodies against either anti-collagen I or II (1:50, Calbiochem), anti-hER (1:200, Santa Cruz) or anti-PH3 (1:100, Upstate) antibodies and the appropriate Alexa 488 secondary antibodies.

Western blotting

For immunoblotting, cells were lysed in 50 mM Tris (pH 7.5), 150 mM NaCl, 0.1% SDS, 0.5% Deoxycholate and 1% Triton X-100 supplemented with a standard protease inhibitor standard mix (1 mM NaF, 1 mM β-glycerophosphate, 5 mM NaPPi, 5 μg/ml Leupeptine, 1 mM Vanadate and 100 μg/ml PMSF). Total protein (50 μg per lane) was separated on a denaturing 12% SDS–PAGE gel and then transferred to PVDF membranes, which were then blocked with 0.1% Tween-20 and 3% low-fat milk in PBS. The membranes were then incubated in the same solution with anti-hER (1:200; Santa Cruz) or anti-total ERK2 (1:500; Santa Cruz) antibodies, and finally with the appropriate horseradish peroxidase-conjugated secondary antibody. Quantification was performed with the L Process v2.0 software from Bioimager Fujifilm.

Quantitative PCR

Quantitative RT–PCR was carried on an ABI PRISM® 7000 sequence detection system using the Syber Green® method. RNA expression was calculated using the comparative Ct method normalised to GAPDH. In experiments on complete bones, data were expressed relative to a calibrator (wild-type mice without tamoxifen) using the $2-(\Delta\Delta Ct) \pm$ s.d. formula. For cell culture experiments, data were normalised using the $C0 \pm$ s.d. formula to compare the relative expression between the different genes. Data are represented as the mean ± s.d. of triplicates from a representative experiment ($n = 3$). ANOVA analysis, $^*P<0.1$, $^{**}P<0.01$, $^{***}P<0.001$.

RT–PCR

Total mRNA (1 μg) was reverse-transcribed using a random primer and Super Script III RT (Promega). PCR was performed with specific primers for mouse *Snail1*, *Runx2* and *Gapdh*. The products amplified were separated in agarose gels and quantified with the L Process v2.0 software from Bioimager Fujifilm.

Promoter analyses

Runx2 promoter activity was measured by cotransfecting primary osteoblast cultures with 50 ng of pcDNA3-Snail1 or empty pcDNA3 vectors and 400 mg of pcL2-Runx2 promoter fragments-Luc. A Renilla reniformis luciferase plasmid (phRL-CMV-Luc from Promega) was also cotransfected as a control for efficiency. Firely and renilla luciferase activity were measured 48 h after transfection using the Dual Luciferase Reporter Assay System (Promega) according to the manufacturer's instructions. The results are presented as the percentage of Luciferase activity relative to control (Luciferase values in cells cotransfected with an empty vector).

ChIP assays

Cells were crosslinked with formaldehyde before DNA sonication. Chromatin was immunoprecipitated with antibodies against rabbit anti-hER (Santa Cruz), anti-H3 (Abcam), as a positive control, or anti-GFP (Invitrogen), as a negative control. In all cases, chromatin was sheared to an average length of 0.5–1 kb. Primers were designed to amplify fragments of 100–200-bp from the mouse *Runx2* promoter containing one of the nine E-boxes or from the mouse *Vdr* promoter containing one of the three E-boxes identified by sequence analysis. The control samples (immunoprecipitated with H3 or GFP antibodies) were amplified with *Gapdh* primers.

Supplementary data

Supplementary figures include the characterisation of transgenic protein nuclear translocation on tamoxifen administration, the analysis of bone mass and bone cells in control animals, the analysis of VDR in the intestine of wild-type and transgenic mice, the effects of the absence of Snail1 on osteoblast proliferation, the analysis of Snail1 binding to distal E-boxes in the *Runx2* promoter and a Table with the sequences of all oligonucleotides used. Supplementary data are available at *The EMBO Journal* Online (http://www.embojournal.org).

Acknowledgements

We thank C Lopez for excellent technical assistance, A Muñoz for kindly providing *Vdr* promoter constructs, MJ Mayol for her help with the serum analyses, all members from M.A. Nieto's lab for helpful discussions and comments and M Sefton for editorial assistance. This work has been supported by the Spanish Ministry of Education and Science (Grants BFU2005-05772, BFU2008-01042, NAN2004-09230-C04-04 and CONSOLIDER-INGENIO 2010 CSD2007-00017) and from the Generalitat Valenciana (Prometeo 2008/049) to MAN. RD is recipient of an INSERM grant.

References

Amling M, Priemel M, Holzmann T, Chapin K, Rueger JM, Baron R, Demay MB (1999) Rescue of the skeletal phenotype of vitamin D receptor-ablated mice in the setting of normal mineral ion homeostasis: formal histomorphometric and biomechanical analyses. *Endocrinology* **140:** 4982–4987

Barrallo-Gimeno A, Nieto MA (2005) The Snail genes as inducers of cell movement and survival: implications in development and cancer. *Development* **132:** 3151–3161

Bialek P, Kern B, Yang X, Schrock M, Sosic D, Hong N, Wu H, Yu K, Ornitz DM, Olson EN, Justice MJ, Karsenty G (2004) A twist code determines the onset of osteoblast differentiation. *Dev Cell* **6:** 423–435

Boutet A, de Frutos CA, Maxwell PH, Mayol MJ, Romero J, Nieto MA (2006) Snail activation disrupts tissue homeostasis and induces fibrosis in the adult kidney. *EMBO J* **25:** 5603–5613

Boyle WJ, Simonet WS, Lacey DL (2003) Osteoclast differentiation and activation. *Nature* **423:** 337–342

Cano A, Perez-Moreno MA, Rodrigo I, Locascio A, Blanco MJ, del Barrio MG, Portillo F, Nieto MA (2000) The transcription factor snail controls epithelial-mesenchymal transitions by repressing E-cadherin expression. *Nat Cell Biol* **2:** 76–83

de Frutos CA, Vega S, Manzanares M, Flores JM, Huertas H, Martinez-Frias ML, Nieto MA (2007) Snail1 is a transcriptional effector of FGFR3 signaling during chondrogenesis and achondroplasias. *Dev Cell* **13:** 872–883

Ducy P, Zhang R, Geoffroy V, Ridall AL, Karsenty G (1997) Osf2/Cbfa1: a transcriptional activator of osteoblast differentiation. *Cell* **89:** 747–754

Hogan B, Beddington R, Constantini F, Lacy E (1994) *Manipulating the mouse embryo A laboratory manual*. Cold Spring Harbor, NY: Cold Spring Harbor Laboratory Press

Jones DC, Wein MN, Oukka M, Hofstaetter JG, Glimcher MJ, Glimcher LH (2006) Regulation of adult bone mass by the zinc finger adapter protein Schnurri-3. *Science* **312:** 1223–1227

Karsenty G, Wagner EF (2002) Reaching a genetic and molecular understanding of skeletal development. *Dev Cell* **2:** 389–406

Kitazawa S, Kajimoto K, Kondo T, Kitazawa R (2003) Vitamin D3 supports osteoclastogenesis via functional vitamin D response element of human RANKL gene promoter. *J Cell Biochem* **89:** 771–777

Komori T (2008) Regulation of bone development and maintenance by Runx2. *Front Biosci* **13:** 898–903

Komori T, Yagi H, Nomura S, Yamaguchi A, Sasaki K, Deguchi K, Shimizu Y, Bronson RT, Gao YH, Inada M, Sato M, Okamoto R, Kitamura Y, Yoshiki S, Kishimoto T (1997) Targeted disruption of Cbfa1 results in a complete lack of bone formation owing to maturational arrest of osteoblasts. *Cell* **89:** 755–764

Kondo T, Kitazawa R, Maeda S, Kitazawa S (2004) 1 alpha,25 dihydroxyvitamin D3 rapidly regulates the mouse osteoprotegerin gene through dual pathways. *J Bone Miner Res* **19:** 1411–1419

Lacey DL, Timms E, Tan HL, Kelley MJ, Dunstan CR, Burgess T, Elliott R, Colombero A, Elliott G, Scully S, Hsu H, Sullivan J, Hawkins N, Davy E, Capparelli C, Eli A, Qian YX, Kaufman S, Sarosi I, Shalhoub V *et al* (1998) Osteoprotegerin ligand is a cytokine that regulates osteoclast differentiation and activation. *Cell* **93:** 165–176

Lagasse E, Weissman IL (1997) Enforced expression of Bcl-2 in monocytes rescues macrophages and partially reverses osteopetrosis in op/op mice. *Cell* **89:** 1021–1031

Li YC, Pirro AE, Amling M, Delling G, Baron R, Bronson R, Demay MB (1997) Targeted ablation of the vitamin D receptor: an animal model of vitamin D-dependent rickets type II with alopecia. *Proc Natl Acad Sci USA* **94:** 9831–9835

Li YC, Pirro AE, Demay MB (1998) Analysis of vitamin D-dependent calcium-binding protein messenger ribonucleic acid expression in mice lacking the vitamin D receptor. *Endocrinology* **139:** 847–851

Maes C, Kobayashi T, Kronenberg HM (2007) A novel transgenic mouse model to study the osteoblast lineage *in vivo*. *Ann N Y Acad Sci* **1116:** 149–164

Masuyama R, Stockmans I, Torrekens S, Van Looveren R, Maes C, Carmeliet P, Bouillon R, Carmeliet G (2006) Vitamin D receptor in chondrocytes promotes osteoclastogenesis and regulates FGF23 production in osteoblasts. *J Clinical Inves* **116:** 3150–3159

Nakashima K, de Crombrugghe B (2003) Transcriptional mechanisms in osteoblast differentiation and bone formation. *Trends Genet* **19:** 458–466

Nakashima K, Zhou X, Kunkel G, Zhang Z, Deng JM, Behringer RR, de Crombrugghe B (2002) The novel zinc finger-containing transcription factor osterix is required for osteoblast differentiation and bone formation. *Cell* **108:** 17–29

Nishio Y, Dong Y, Paris M, O'Keefe RJ, Schwarz EM, Drissi H (2006) Runx2-mediated regulation of the zinc finger Osterix/Sp7 gene. *Gene* **372:** 62–70

Ornitz DM, Marie JP (2002) FGF signaling pathways in endochondral and intramembranous bone development and human genetic disease. *Genes Dev* **16:** 1446–1465

Otto F, Thornell AP, Crompton T, Denzel A, Gilmour KC, Rosewell IR, Stamp GW, Beddington RS, Mundlos S, Olsen BR, Selby PB, Owen MJ (1997) Cbfa1, a candidate gene for cleidocranial dysplasia syndrome, is essential for osteoblast differentiation and bone development. *Cell* **89:** 765–771

Palmer HG, Larriba MJ, Garcia JM, Ordonez-Moran P, Pena C, Peiro S, Puig I, Rodriguez R, de la Fuente R, Bernad A, Pollan M, Bonilla F, Gamallo C, de Herreros AG, Munoz A (2004) The transcription factor SNAIL represses vitamin D receptor expression and responsiveness in human colon cancer. *Nat Med* **10:** 917–919

Panda DK, Miao D, Bolivar I, Li J, Huo R, Hendy GN, Goltzman D (2004) Inactivation of the 25-hydroxyvitamin D 1alpha-hydroxylase and vitamin D receptor demonstrates independent and interdependent effects of calcium and vitamin D on skeletal and mineral homeostasis. *J Biol Chem* **279:** 16754–16766

Parfitt AM, Drezner MK, Glorieux FH, Kanis JA, Malluche H, Meunier PJ, Ott SM, Recker RR (1987) Bone histomorphometry: standardization of nomenclature, symbols, and units. Report of the ASBMR Histomorphometry Nomenclature Committee. *J Bone Miner Res* **2:** 595–610

Peinado H, Olmeda D, Cano A (2007) Snail, Zeb and bHLH factors in tumour progression: an alliance against the epithelial phenotype? *Nat Rev Cancer* **7:** 415–428

Pena C, Garcia JM, Silva J, Garcia V, Rodriguez R, Alonso I, Millan I, Salas C, de Herreros AG, Munoz A, Bonilla F (2005) E-cadherin and vitamin D receptor regulation by SNAIL and ZEB1 in colon cancer: clinicopathological correlations. *Hum Mol Genet* **14:** 3361–3370

Reyes M, Lund T, Lenvik T, Aguiar D, Koodie L, Verfaillie CM (2001) Purification and *ex vivo* expansion of postnatal human marrow mesodermal progenitor cells. *Blood* **98:** 2615–2625

Rodan GA, Martin TJ (2000) Therapeutic approaches to bone diseases. *Science* **289:** 1508–1514

Simonet WS, Lacey DL, Dunstan CR, Kelley M, Chang MS, Lüthy R, Nguyen HQ, Wooden S, Bennett L, Boone T, Shimamoto G, DeRose M, Elliott R, Colombero A, Tan HL, Trail G, Sullivan J, Davy E, Bucay N, Renshaw-Gegg L *et al* (1997) Osteoprotegerin: a novel secreted protein involved in the regulation of bone density. *Cell* **89:** 309–319

Stein GS, Lian JB, van Wijnen AJ, Stein JL, Montecino M, Javed A, Zaidi SK, Young DW, Choi JY, Pockwinse SM (2004) Runx2 control of organization, assembly and activity of the regulatory machinery for skeletal gene expression. *Oncogene* **23:** 4315–4329

Vega S, Morales AV, Ocaña OH, Valdes F, Fabregat I, Nieto MA (2004) Snail blocks the cell cycle and confers resistance to cell death. *Genes Dev* **18:** 1131–1143

Woods A, Beier F (2006) RhoA/ROCK signaling regulates chondrogenesis in a context-dependent manner. *J Biol Chem* **281:** 13134–13140

Wu K, Willett WC, Fuchs CS, Colditz GA, Giovannucci EL (2002) Calcium intake and risk of colon cancer in women and men. *J Natl Cancer Inst* **94:** 437–446

Xiao G, Jiang D, Ge C, Zhao Z, Lai Y, Boules H, Phimphilai M, Yang X, Karsenty G, Franceschi RT (2005) Cooperative interactions between activating transcription factor 4 and Runx2/Cbfa1 stimulate osteoblast-specific osteocalcin gene expression. *J Biol Chem* **280:** 30689–30696

Yoshizawa T, Handa Y, Uematsu Y, Takeda S, Sekine K, Yoshihara Y, Kawakami T, Arioka K, Sato H, Uchiyama Y, Masushige S, Fukamizu A, Matsumoto T, Kato S (1997) Mice lacking the vitamin D receptor exhibit impaired bone formation, uterine hypoplasia and growth retardation after weaning. *Nat Genet* **16:** 391–396

